Optical tactile sensor using scattering inside sol–gel-derived flexible macroporous monoliths

Gen Hayase

International Center for Materials Nanoarchitectonics, National Institute for Materials Science, 1-1 Namiki Tsukuba, Ibaraki 305-0044, Japan

*Email: gen@aerogel.jp

Highlights

- A tactile sensor was fabricated using Mie scattering inside a flexible monolith.
- Compressing the porous material reduced the amount of light detected.
- The materials are available for sensors less than 1 mm.

Abstract

Tactile sensors are an essential technology for robots, and various types have been developed. This paper reports on a new optical tactile sensor based on multiple scattering in a porous material with a viscoelastic phase-separated structure fabricated by a sol‑gel method. When a macroporous silicone monolith with a few micrometer diameter skeletons was compressed, the diffuse light intensity near the light source was reduced due to Mie multiple scattering. This light intensity change was opposite to the behavior of conventional polymer foams (cellular structures), which have a large structural scale. A simple tactile sensor using a macroporous monolith and a photo reflector was fabricated based on this finding. The skeleton diameter was an important factor for the sensor. In the case of macroporous silicones, the voltage-strain curve showed an almost hysteresis-free clear response. However, the response of macroporous polymethylmethacrylate monolith with a smaller skeleton diameter was weak due to low Mie scattering intensity. Sensors using sol–gel derived macroporous materials have the potential to be thinner and provide improved surface tactile sensation compared to foam materials.

Graphical Abstract

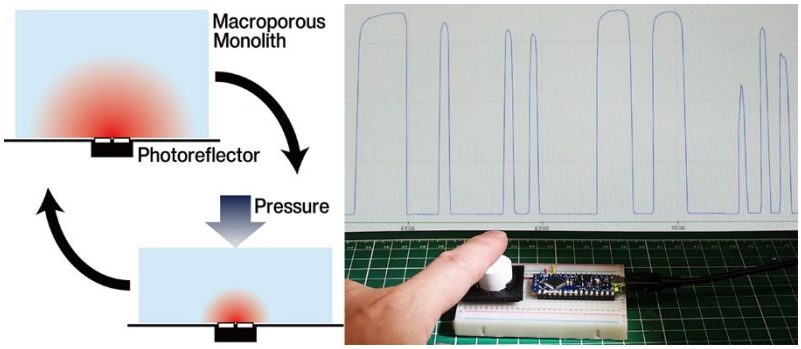

Keywords

sol–gel, silicone, macroporous monoliths, flexible, Mie scattering, optical tactile sensor

1 Introduction

The development of engineering technology has led to the widespread use of robots. In experimental research, the use of collaborative robots to reduce labor for routine tasks has increased, and attempts have been made to automate cell culture and analytical measurements. Various types of sensors are required to operate robots accurately and safely. Tactile sensors are essential for precise movements, such as accurately holding an object with a robot gripper, and various sensors have been devised.[1-3] One widely used sensor utilizes wires stretched in a mesh-like pattern to detect resistance in a membrane.[4-9] Low-cost sheet-type sensors are used for pressure-sensing applications other than robotics. In material chemistry, materials whose conductivity changes with deformation have been extensively developed. Composites of conductive materials added to flexible insulating ones can be used as highly durable sensors with elasticity.[10-12] For example, conductive sponges used to protect semiconductor electronic components were reported to be utilized as pressure sensors 40 years ago.[13] Improvements continue to be made using various materials, and especially in the last decade, composites of two-dimensional nanomaterials have been investigated to increase pressure sensitivity.[14-18] Optical sensors using elastomers have also been developed to measure pressure distribution and surface topography of objects in contact.[19] Those tactile sensors have advantages and disadvantages in terms of mechanical properties, durability, sensitivity, etc.[20] Different types of sensors are used in different manners depending on the application. If a wide variety of sensors are developed, it will be possible to select the most suitable sensor for each application.[21]

Our group has studied flexible silicone macroporous materials fabricated using the

continuous phase-separated structure generated during liquid-phase reactions.[22-24] Generally, macroporous materials prepared using the sol–gel method have finer pores and skeletal microstructures than three-dimensional cellular structures such as foams.[25, 26] Our material has a porosity of over 90 %, and it shows high flexibility in combination with the mechanical properties of silicone. Marshmallow-like gels (MGs) are white because of their microstructure because light incident on an MG is multiply scattered (Mie scattering) by several micrometer-diameter frameworks, while the dense silicone is colorless and transparent. The compression of the MG does not cause any color change. However, as the microstructure changes during deformation, the light scattering inside the material should change. I hypothesized that a simple tactile sensor could be fabricated by detecting this change.

Optical sensors utilizing the changes in reflectance and transmittance in the flexible porous framework have been developed and commercialized.[27, 28] However, there have been no reports on sensors utilizing multiple scattering attenuation to the best of our knowledge because flexible porous materials with a structural scale similar to MGs are relatively new materials. Neither materials researchers nor sensor developers have focused on this application. This paper presents the characteristics of a sensor that utilizes the changes in the intensity of multiple scattered lights inside MGs. Furthermore, I discuss the general conditions for fabricating optical sensors using flexible porous materials by examining the response of the sensors that use porous polymethylmethacrylate (PMMA) and melamine sponges.

2 Experimental

2.1 Materials

Methyltrimethoxysilane (MTMS), dimethyldimethoxysilane (DMDMS), and *n*-hexadecyltrimethylammonium chloride (CTAC), were purchased from Tokyo Chemical Industry Co., Ltd. (Japan). Acetic acid, urea, methanol, ethanol, 2-propanol, and glycerol were purchased from Kanto Chemical Co., Inc. (Japan). PMMA (average Mw ~ 350,000) was purchased from Merck KGaA (Germany). All reagents were used as received.

2.2 Sample preparation of MGs

Macroporous silicone monoliths (MGs) were prepared based on previous studies.[29] First, x mL of 5 mM acetic acid was dissolved in a glass tube with 1.0 g of CTAC and $0.33 \cdot x$ g of urea at

room temperature (RT ~22 °C). 3.0 mL of MTMS and 2.0 mL of DMDMS were added to this solution, and the mixture was stirred well for 15 min at RT. The resulting sol was placed in a sealed cylindrical perfluoroalkoxy (PFA) container and heated at 80 °C for 12 h for gelation and aging. The gel was removed from the container, immersed in methanol at RT for several hours and several times to wash the interior. Then, it was evaporated and dried at 50 °C to obtain the target product named MG*x*.

2.3 Sample preparation of PMMA monolith

According to a previous report,[30] 10 mL of a mixture of 80 % ethanol and 20 % water (by volume) in a 20 mL glass tube was maintained at 80 °C, and 0.40 g of PMMA powder was added and dissolved while stirring well. After confirming that the PMMA was completely dissolved, the vial containing the sol was allowed to stand and cool at 20 °C to gelatinize. The resulting wet gel was immersed in a sufficient amount of water for 8 h × 2 times for washing and then immersed in an aqueous solution containing 5 % glycerin as a plasticizer for solvent exchange. Finally, macroporous PMMA monoliths were obtained by vacuum drying at RT.

2.4 Melamine sponge

A commercially available melamine sponge (Gekiochikun-Cube S00558, LEC, Inc., Japan; Basotect W, BASF SE, Germany) was used.

2.5 Sensor assembly

A photoreflector module (QTR-1A, Pololu Corporation, USA) was embedded in a substrate fabricated by a three-dimensional printer, and then, a monolithic porous material was placed on it. The change in the light intensity at an infrared wavelength of 940 nm was output as an analog electric potential value. For multipoint sensing, four circuits identical to the photo reflector module were arranged on an electronic board.

2.6 Evaluation of macroporous monoliths and sensors

The bulk density of the macroporous monoliths was calculated from the measured weight and volume. The microstructure of the materials was observed using a scanning electron microscope (TM3000, Hitachi High-Technologies Corporation, Japan). ImageJ2/Fiji was used for scale

analysis.[31, 32] The skeletal diameter was determined by averaging from about 20 randomly selected locations. Light absorbance was measured using a UV-VIS-IR spectrometer (V-770). In addition, an integrating sphere (ISN-923, JASCO Corporation, Japan) was used to obtain the diffuse reflection relative to the white diffuse reflectance standard (polytetrafluoroethylene). A self-made device was used to measure the change in the light intensity when MG15 was compressed to 50 %. Optical fibers were placed under the sample. The distance between the emitting and detecting points was 5 mm. A halogen light source (KTX-100E, KenkoTokina Corporation, Japan) and a mini-spectrometer (C13555MA, Hamamatsu Photonics K.K., Japan) were used for the measurements. Uniaxial compression tests were performed using a universal tensile testing machine (EZ-SX, Shimadzu Corporation, Japan) and a 500 N pressure gauge. The tactile sensor was connected to the analog input terminal of the testing machine to read the electric potential values. Sensor response speed was analyzed using a high-speed industrial camera (VCXU-02M, Baumer, Switzerland).

3 Results and Discussion

3.1 Change in light scattering due to marshmallow-like gel compression and wavelength of sensor

Marshmallow-like gels (MGs) and PMMA monoliths were prepared as the macroporous materials for the sensors in this study based on existing methods. The physical properties of the prepared materials are shown in Table 1. First, the properties of MG15 were investigated for optical sensors.

Table 1. Physical properties of materials used in optical tactile sensors.

	Bulk density/g cm^{-3}	Young's modulus/kPa	Skeletal diameter/μm
MG10	0.15	22	5
MG15	0.11	5.0	4
MG20	0.091	3.6	3
PMMA monolith	0.17	720	0.3
Melamine sponge	0.0077	14	10

A simple test was used to observe the change in scattered light caused by the compression of MG15. When cylindrical MG15 was placed on an LED array and pressed with a

finger, the light intensity decreased. This change could be because light scattering inside the material reduced the side scattering intensity (Figure 1). The principle of this phenomenon is that particles with a size similar to the wavelength of light cause strong Mie scattering. Although MG15 had a continuous framework, viscoelastic phase-separated structures,[33, 34] such as fused spherical particles, were prone to Mie scattering (Figure 2a). When MG15 was compressed, porosity decreased, and the fraction of skeletons in the space increased. In contrast, the skeleton diameter remained almost unchanged. Thus, the compression of the monolith increased the scattering source density. Mie scattering is more likely to occur when scattering sources increase and observed light becomes more attenuated by interference. Thus, as MG15 compression increased, the light intensity observed at the monolith exterior decreased.

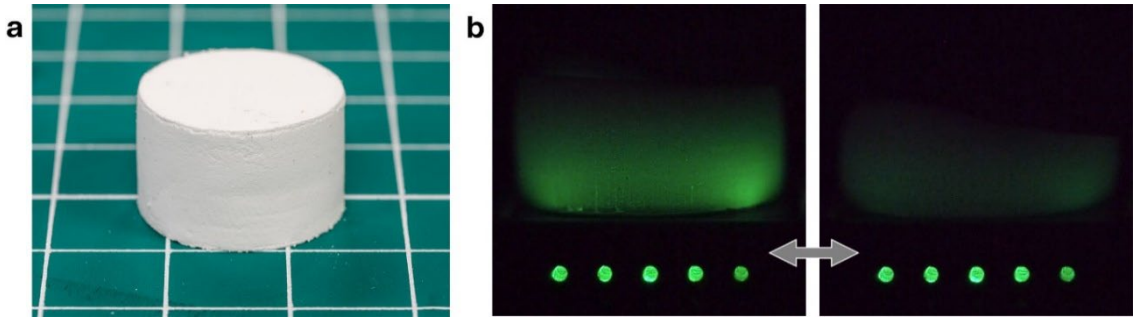

Figure 1. (a) Cylindrical MG15 with a diameter of 17 mm and a height of 10 mm. (b) Change in appearance before and after pressing MG15 on the green LED array. See also Movie S1, Supplementary material.

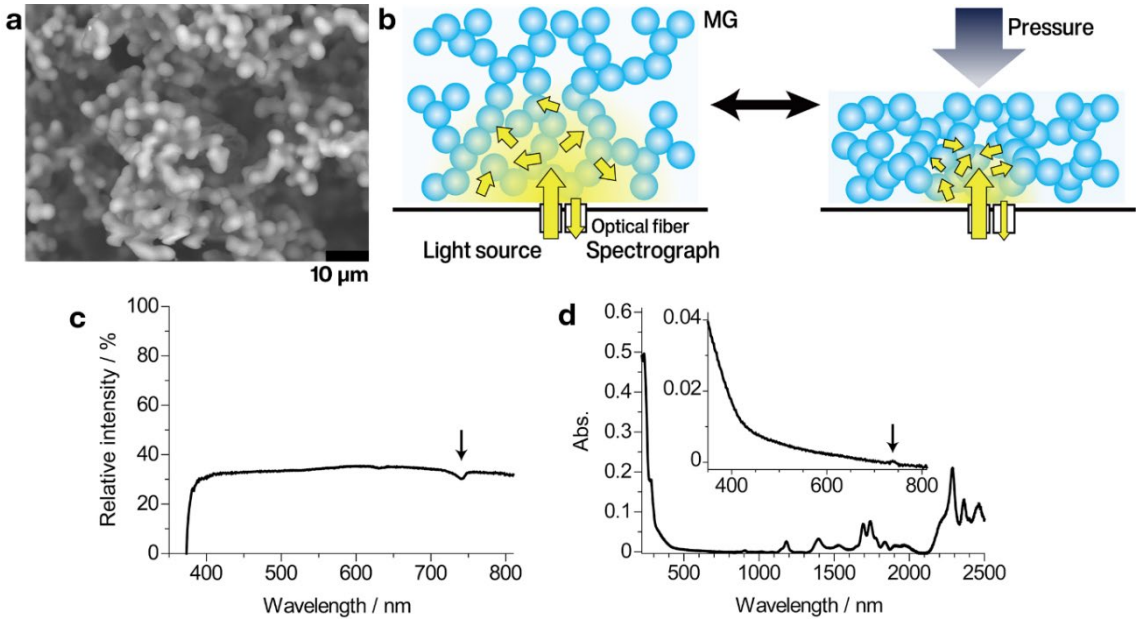

Figure 2. (a) SEM image of MG15. (b) Schematic of the apparatus used for spectral measurements during compression of MG15. (c) Relative light intensity at 50 % compression of MG relative to uncompressed. (d) Absorbance of MG15 surface obtained by a total light reflectance measurement. The slight peak indicated by the arrow at 740 nm corresponds to the arrow in (c).

I assembled an optical apparatus to quantitatively examine the changes in the light intensity before and after compression, as shown in Figure 2b. Optical fibers connected to a halogen light source and a small monochromator were installed on a substrate, and the change in the visible light range was investigated when MG15 was compressed by 50 %. At wavelengths above 400 nm, the light intensity after compression was 30–35 % of the light intensity before compression. However, at wavelengths below 400 nm, the light intensity after compression decreased significantly. Moreover, a slight change was observed around 745 nm (Figure 2c). These changes occurred because the silicone skeleton of MG15 absorbed light at specific wavelengths (Figure 2d). Regarding the detectable deformation range, selecting a wavelength that is less likely to cause optical absorption to use MGs as sensor components is necessary. From the total light reflectance measurement, a wavelength range of 400–1100 nm is appropriate, which is almost the same as the photosensitive range of Si photodiodes.

3.2 Fabrication of miniature optical tactile sensor using marshmallow-like gel and compression response

The macroporous monoliths were used to fabricate a small optical tactile sensor by utilizing a photoreflector with a 940 nm IR LED and a silicon photodiode. The sensor had a simple structure with monoliths placed on a commercial photoreflector module. Nevertheless, it could rapidly detect changes in response to compression when tested using a single-board microcontroller (Figure S1 and Movie S2, the sample code in Supplementary material). Additionally, multipoint sensing was performed by placing multiple photoreflectors on the substrate (Figure 3, Figures S2, S3, and Movies S3, S4 in Supplementary material). This system enabled us to perform the same three-dimensional measurement as is done with commercially available transmissive sensors using flexible sponges.

The relationship between the strain, stress, and potential of a sensor that used MG15 as a component was investigated using a mechanical testing apparatus. The component configuration and circuit diagram of this sensor are shown in Figure 4a and b. Figure 4c-f shows the results of 10 cycles of 10 s of loading, 10 s of unloading, and 10 s of standing still at 0–50 % strain. Because this sensor was just an MG15 on a photo reflector, the first few cycles of readings were somewhat erratic. This is because the MG15 is flexible and has an uneven surface of several tens of micrometers, and it takes time for the bottom surface shape to stabilize. However, once stabilized, the curves were nearly identical. Figure 4 shows the test results up to the 10th cycle, but at least a few hundred cycles showed the same results as the 10th cycle curve. Once this response stabilized, the curve did not change significantly when the test was paused and restarted after several hours. Hysteresis was observed in the stress–strain curve during loading and unloading because of the viscoelasticity of the MG15. Furthermore, there was negligible hysteresis in the potential–strain curve during loading and unloading because structural changes caused the scattering in MG15. Even between the different monoliths, the curves were nearly identical after a few cycles. When a compressed MG15 is unloaded, the stress recovery is slower, while the external shape quickly returns to normal. For example, instantaneous unloading from 50% compression results in zero displacement after 50 ms at the latest. When compressed, detection is possible within 10 ms. This response speed is considered sufficient for contact detection, for example. Similar mechanical test results were obtained when MGs with different Young's moduli were used (Figure 5). The potential changed significantly below ~5 % distortion in all three cases and showed a gentle and almost linear change for 10–40 % distortion. Although there was a slight difference, the curve on the graph was smoother when MG15 was tested than when other samples

were used. This difference should be because MG15 was prepared under optimal conditions and had fewer by-products and less drying shrinkage during fabrication than the different samples.[29]

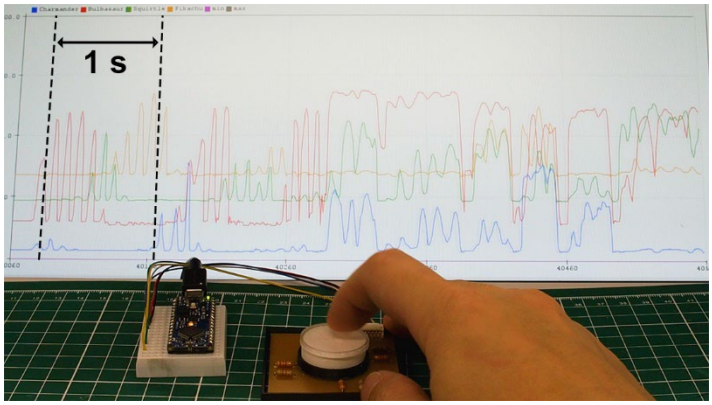

Figure 3. Multipoint sensing using MG15 and four photoreflectors. See also Figures S2, S3 and Movies S3, S4, Supplementary material.

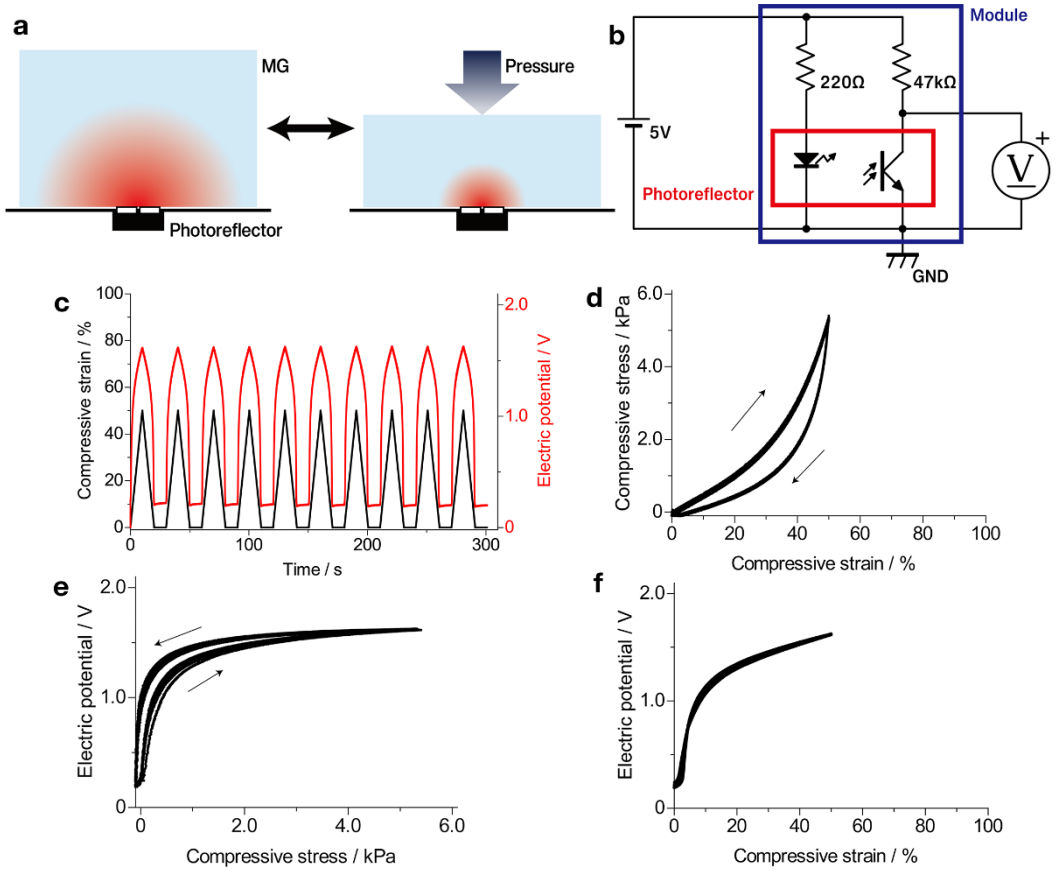

Figure 4. (a) Schematic of the optical tactile sensor. (b) Circuit diagram of the sensor used for the mechanical measurement. (c) Strain and potential changes during the measurement. (d) Stress-

strain curve of MG15 for 10 cycles. (e) Potential-stress curve and (f) potential-strain curve for 10 cycles. Semilog plots of Figure 4e and f are available in Figure S4 in Supplementary material.

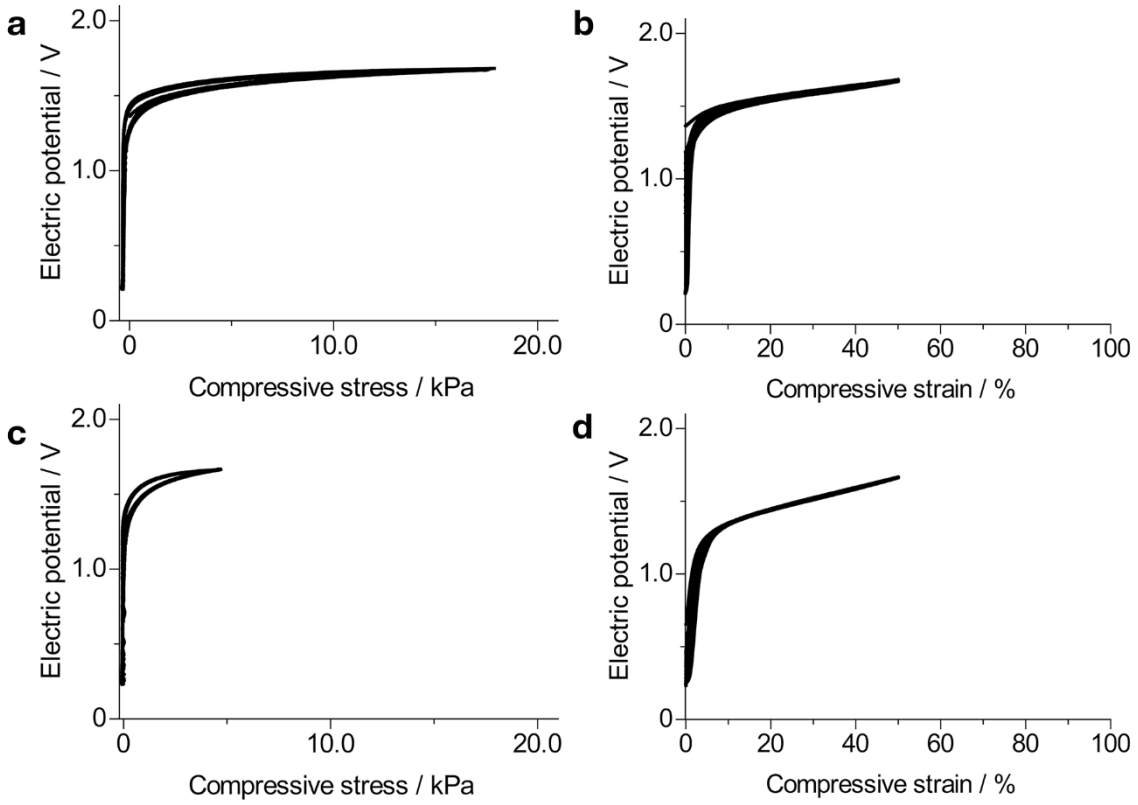

Figure 5. (a) Potential–stress and (b) potential–strain curves of MG10. (c) Potential–stress and (d) potential–strain curves for MG20. All graphs are overlaid with test results from 10 cycles of compression-unloading. The curves from a few cycles later to the 100th cycle (not shown in this figure) were almost identical in each result. Semilog plots are available in Figure S4 in Supplementary material.

3.3 Evaluation of sensor with polymethylmethacrylate monolith and melamine sponge as tactile sensing parts

I attempted to fabricate similar sensors using flexible monolithic macroporous materials other than MGs. Polymethylmethacrylate (PMMA) monoliths are macroporous materials easily fabricated via the sol–gel reaction with thermally induced phase separation.[30, 35] They have a flexible continuous granular skeleton but are not as flexible as MGs. Mechanical tests were conducted using this porous material as a tactile sensor component. As the PMMA monolith had a low deformation rate, I conducted tests in the range of 0–10 % of strain for 30 s of loading and

30 s of unloading and found that the potential changed according to the amount of strain (Figure 6a-c). However, the change was smaller compared to MG15. This difference was because the skeleton diameter of the PMMA monolith was smaller than that of MG15 (Figure 6d), resulting in lower scattering intensity.

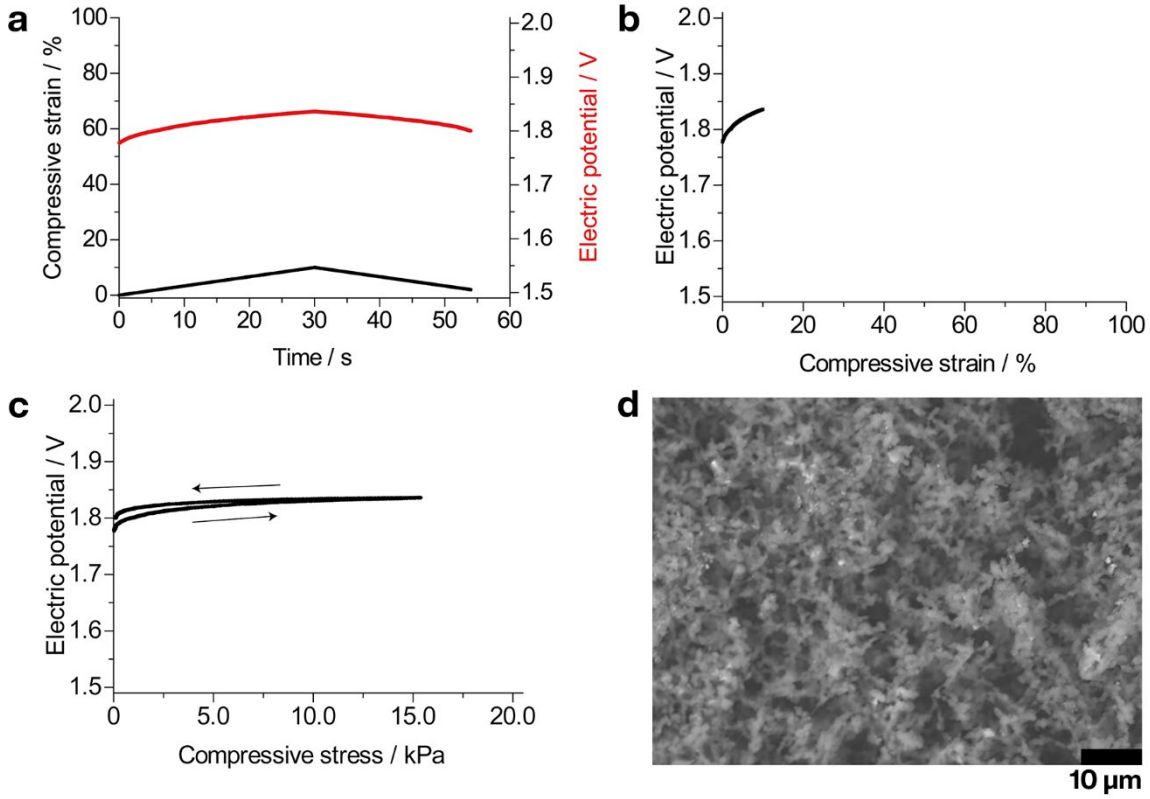

Figure 6. (a) Strain and potential change during measurement in a sensor with the PMMA monolith. (b) Potential–stress and (c) potential–strain curves of the PMMA monolith. (d) SEM image of the PMMA monolith. Semilog plots of Figure 6b and c are available in Figure S4 in Supplementary material.

When the melamine sponge and urethane foam were used as a flexible optical component, the test results differed from the MGs and PMMA monoliths, which caused a negative potential change in response to compression. Figure 7 shows the cycle test results at the same deformation rate as MG15. Similar results have been reported in previous studies using urethane foam and photoreflectors.[28] Melamine sponges have cellular structures formed by foaming, and the scale of their framework and pore structure is one order of magnitude larger than the wavelength of light used in the sensor (Figure 7d). Mie scattering is more likely to occur in the

skeleton of the monoliths formed by phase separation, whereas the relatively large rod-like structure of the cellular network is more likely to cause reflection near the light source. When melamine sponges or urethane foams are compressed, more light is reflected close to the light source, resulting in a stronger intensity observed by the photodetector. Therefore, the cellular and phase-separated structures change the light intensity detected by the photoreflector owing to deformation by different mechanisms.

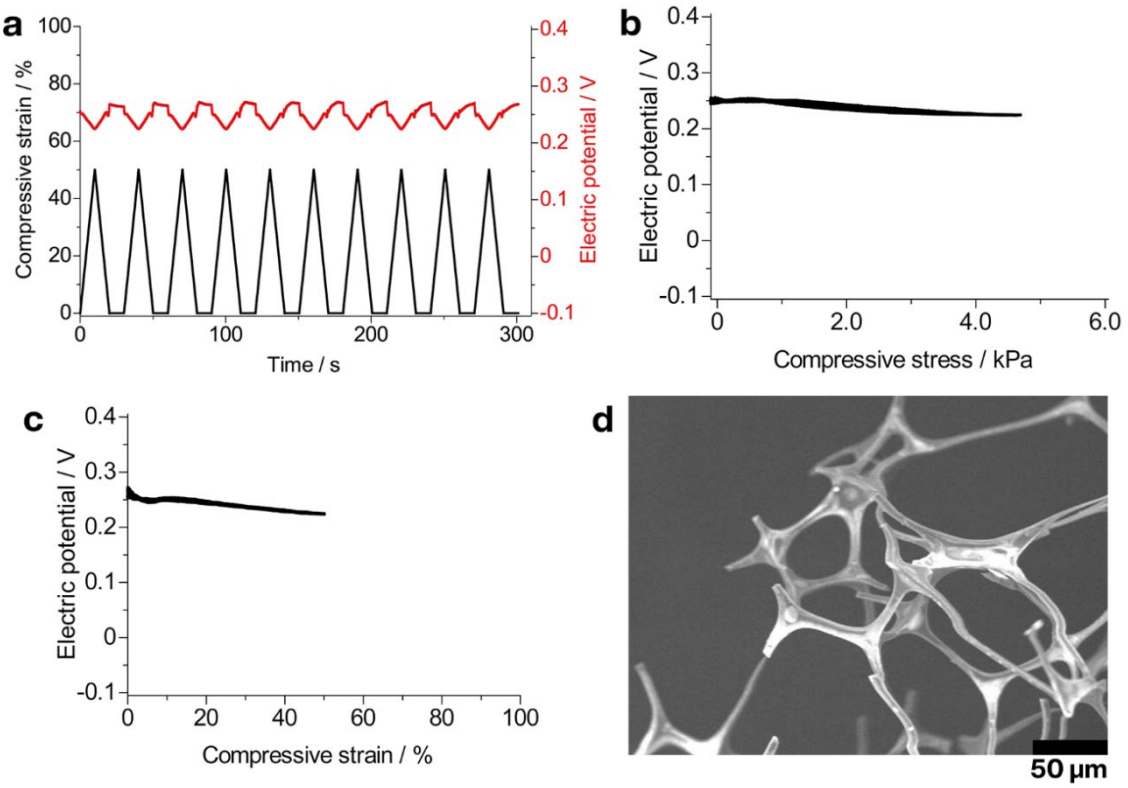

Figure 7. (a) Strain and potential change during measurement in a sensor with the melamine sponge. (b) Potential–stress and (c) potential–strain curves of the melamine sponge for 10 cycles. (d) SEM image of the melamine sponge.

The advantage of macroporous materials with phase-separated structures is that they can change the light intensity even in small and thin bulk. MG15 works well at a thickness of less than 1 mm (Movie S5, Supplementary material), where the melamine sponge and urethane foam allow for considerable light penetration. The porous silicone surface is almost 100 % reflective (Figure 2d), allowing almost no light from the outside to penetrate. Furthermore, differences in structure affect the tactile feel as an interface. These features are expected to be applied to grippers

with thin and flexible skin (Movie S6, Supplementary material). Future research on fabricating flexible monolithic porous materials with different compositions can provide a better understanding of the response characteristics of tactile sensors and other interface textures.

4 Conclusion

The compression of sol–gel-derived monolithic macroporous materials decreased backscattering intensity because of absorption and multiple scattering. When MG15 was compressed by 50 % relative to its total height, the light intensity around the light source decreased to 30 % of that before compression. This phenomenon was used to fabricate a simple tactile sensor by placing MGs on a photoreflector, which changed its electric potential upon compression. Multipoint sensing was achieved by increasing the number of photoreflectors. The sensor exhibited negligible hysteresis in the potential–strain curve but hysteresis in the potential–stress curve because of its viscoelasticity. When the PMMA monolith was used instead of MGs as an interface, a similar change in the light intensity was detected in response to compression. However, the magnitude of the change was smaller. This difference was because the skeletal structure was smaller than the optical wavelength and light scattering was less likely to occur. In contrast, when a melamine sponge with a cell structure was used as the sensor component, the detected light intensity increased with compression. This change was because the amount of light reflected in the vicinity of the light source by the skeleton increases with compression in cell structures with a scale of one order of magnitude larger than the wavelength of light. The advantage of macroporous materials produced using the sol–gel method over cellular networks is that they can change the light intensity even in bulk with a thickness of less than 1 mm. The development of other flexible porous materials with skeletal diameters close to the wavelength of light can expand the applications of this optical sensor.

Declaration of Competing Interest

The author declares no conflict of interest.

Acknowledgements

This research was supported by MEXT Leading Initiative for Excellent Young Researchers (LEADER).

References

[1] H. Yousef, M. Boukallel, K. Althoefer, Tactile sensing for dexterous in-hand manipulation in robotics-A review, Sens Actuators A: Phys, 167(2011) 171-187. https://doi.org/10.1016/j.sna.2011.02.038

[2] R.S. Dahiya, G. Metta, M. Valle, G. Sandini, Tactile Sensing-From Humans to Humanoids, IEEE Trans Robot, 26(2010) 1-20. https://doi.org/10.1109/tro.2009.2033627

[3] O. Kerpa, K. Weiss, H. Worn, Ieee, Development of a flexible tactile sensor system for a humanoid robot, Proceedings 2003 IEEE/RSJ International Conference on Intelligent Robots and Systems (IROS 2003), 1(2003) 1-6. https://doi.org/10.1109/iros.2003.1250596

[4] K. Bae, J. Jeong, J. Choi, S. Pyo, J. Kim, Large-Area, Crosstalk-Free, Flexible Tactile Sensor Matrix Pixelated by Mesh Layers, ACS Appl Mater Interfaces, 13(2021) 12259-12267. https://doi.org/10.1021/acsami.0c21671

[5] F. Sygulla, F. Ellensohn, A.C. Hildebrandt, D. Wahrmann, D. Rixen, Ieee, A Flexible and Low-Cost Tactile Sensor for Robotic Applications, IEEE International Conference on Advanced Intelligent Mechatronics (AIM), Munich, Germany, 2017, pp. 58-63.

[6] G.H. Buscher, R. Koiva, C. Schurmann, R. Haschke, H.J. Ritter, Flexible and stretchable fabric-based tactile sensor, Rob Auton Syst, 63(2015) 244-252. https://doi.org/10.1016/j.robot.2014.09.007

[7] M. Shimojo, A. Namiki, M. Ishikawa, R. Makino, K. Mabuchi, A tactile sensor sheet using pressure conductive rubber with electrical-wires stitched method, IEEE Sens J, 4(2004) 589-596. https://doi.org/10.1109/jsen.2004.833152

[8] R. Li, G.X. Chen, M.H. He, J.F. Tian, B. Su, Patternable transparent and conductive elastomers towards flexible tactile/strain sensors, J Mater Chem C, 5(2017) 8475-8481. https://doi.org/10.1039/c7tc02703f

[9] S. Gong, W. Schwalb, Y.W. Wang, Y. Chen, Y. Tang, J. Si, et al., A wearable and highly sensitive pressure sensor with ultrathin gold nanowires, Nat Commun, 5(2014) 3132. https://doi.org/10.1038/ncomms4132

[10] J.H. Oh, J.Y. Woo, S. Jo, C.S. Han, Pressure-conductive rubber sensor based on liquid-metal-PDMS composite, Sens Actuators A: Phys, 299(2019) 111610. https://doi.org/10.1016/j.sna.2019.111610

[11] M. wKnite, V. Teteris, A. Kiploka, J. Kaupuzs, Polyisoprene-carbon black nanocomposites as tensile strain and pressure sensor materials, Sens Actuators A: Phys, 110(2004) 142-149. https://doi.org/10.1016/j.sna.2003.08.006

[12] M. Hussain, Y.H. Choa, K. Niihara, Conductive rubber materials for pressure sensors, J Mater Sci Lett, 20(2001) 525-527. https://doi.org/10.1023/a:1010972315505

[13] T. Henry, Conductive Foam Forms Reliable Pressure Sensor, Electronics, 55(1982) 161-163.
[14] Z.G. Wu, L.S. Wei, S.W. Tang, Y.T. Xiong, X.Q. Qin, J.W. Luo, et al., Recent Progress in Ti3C2TX MXene-Based Flexible Pressure Sensors, ACS Nano, 15(2021) 18880-18894. https://doi.org/10.1021/acsnano.1c08239
[15] Y. Pang, H. Tian, L.Q. Tao, Y.X. Li, X.F. Wang, N.Q. Deng, et al., Flexible, Highly Sensitive, and Wearable Pressure and Strain Sensors with Graphene Porous Network Structure, ACS Appl Mater Interfaces, 8(2016) 26458-26462. https://doi.org/10.1021/acsami.6b08172
[16] H. Tian, Y. Shu, X.F. Wang, M.A. Mohammad, Z. Bie, Q.Y. Xie, et al., A Graphene-Based Resistive Pressure Sensor with Record-High Sensitivity in a Wide Pressure Range, Sci Rep, 5(2015) 8603. https://doi.org/10.1038/srep08603
[17] H.B. Yao, J. Ge, C.F. Wang, X. Wang, W. Hu, Z.J. Zheng, et al., A Flexible and Highly Pressure-Sensitive Graphene-Polyurethane Sponge Based on Fractured Microstructure Design, Adv Mater, 25(2013) 6692-6698. https://doi.org/10.1002/adma.201303041
[18] S. Brady, D. Diamond, K.T. Lau, Inherently conducting polymer modified polyurethane smart foam for pressure sensing, Sens Actuators A: Phys, 119(2005) 398-404. https://doi.org/10.1016/j.sna.2004.10.020
[19] M. Lambeta, P.W. Chou, S. Tian, B. Yang, B. Maloon, V.R. Most, et al., DIGIT: A Novel Design for a Low-Cost Compact High-Resolution Tactile Sensor With Application to In-Hand Manipulation, IEEE Robot Autom Lett, 5(2020) 3838-3845. https://doi.org/10.1109/lra.2020.2977257
[20] M.L. Hammock, A. Chortos, B.C.K. Tee, J.B.H. Tok, Z.A. Bao, 25th Anniversary Article: The Evolution of Electronic Skin (E-Skin): A Brief History, Design Considerations, and Recent Progress, Adv Mater, 25(2013) 5997-6037. https://doi.org/10.1002/adma.201302240
[21] Y.B. Wan, Y. Wang, C.F. Guo, Recent progresses on flexible tactile sensors, Mater Today Phys, 1(2017) 61-73. https://doi.org/10.1016/j.mtphys.2017.06.002
[22] G. Hayase, S.-i.M. Nomura., Macroporous Silicone Sheets Integrated with Meshes for Various Applications, ACS Appl Polym Mater, 1(2019) 2077-2082. https://doi.org/10.1021/acsapm.9b00382
[23] G. Hayase, K. Kanamori, M. Fukuchi, H. Kaji, K. Nakanishi, Facile Synthesis of Marshmallow-like Macroporous Gels Usable under Harsh Conditions for the Separation of Oil and Water, Angew Chem Int Ed, 52(2013) 1986-1989. https://doi.org/10.1002/anie.201207969
[24] G. Hayase, K. Kanamori, K. Nakanishi, New Flexible Aerogels and Xerogels Derived from Methyltrimethoxysilane/Dimethyldimethoxysilane Co-precursors, J Mater Chem, 21(2011) 17077-17079. https://doi.org/10.1039/c1jm13664j
[25] L.J. Gibson, M.F. Ashby, Cellular Solids: Structure and Properties, 2nd Edition ed., Cambridge, UK: Cambridge University Press; 1999.

[26] C.J. Brinker, G.W. Scherer, Sol-Gel Science: The Physics and Chemistry of Sol-Gel Processing, San Diego: Academic Press; 1990.
[27] A. Nagano, T. Watanabe, N. Maruyama, Flexible tactile sensor, Japanese Patent JP5722259B2, 2015.
[28] Y. Ohmura, Y. Kuniyoshi, A. Nagakubo, Conformable and scalable tactile sensor skin for curved surfaces, IEEE International Conference on Robotics and Automation (ICRA), Orlando, FL, 2006, pp. 1348-1353.
[29] G. Hayase, Y. Ohya, Marshmallow-like Silicone Gels as Flexible Thermal Insulators and Liquid Nitrogen Retention Materials and Their Application in Containers for Cryopreserved Embryos, Appl Mater Today, 9(2017) 560-565. https://doi.org/10.1016/j.apmt.2017.10.004
[30] S. Yoneda, W.J. Han, U. Hasegawa, H. Uyama, Facile fabrication of poly(methyl methacrylate) monolith via thermally induced phase separation by utilizing unique cosolvency, Polymer, 55(2014) 3212-3216. https://doi.org/10.1016/j.polymer.2014.05.031
[31] C.T. Rueden, J. Schindelin, M.C. Hiner, B.E. DeZonia, A.E. Walter, E.T. Arena, et al., ImageJ2: ImageJ for the Next Generation of Scientific Image Data, BMC Bioinform, 18(2017) 529529. https://doi.org/10.1186/s12859-017-1934-z
[32] J. Schindelin, I. Arganda-Carreras, E. Frise, V. Kaynig, M. Longair, T. Pietzsch, et al., Fiji: An Open-source Platform for Biological-image Analysis, Nat Methods, 9(2012) 676-682. https://doi.org/10.1038/nmeth.2019
[33] H. Tanaka, Viscoelastic Phase Separation, J Phys Condens Matter, 12(2000) R207-R264. https://doi.org/10.1088/0953-8984/12/15/201
[34] A. Surendran, J. Joy, J. Parameswaranpillai, S. Anas, S. Thomas, An overview of viscoelastic phase separation in epoxy based blends, Soft Matter, 16(2020) 3363-3377. https://doi.org/10.1039/c9sm02361e
[35] K. Okada, M. Nandi, J. Maruyama, T. Oka, T. Tsujimoto, K. Kondoh, et al., Fabrication of mesoporous polymer monolith: a template-free approach, Chem Commun, 47(2011) 7422-7424. https://doi.org/10.1039/c1cc12402a

Vitae

Gen Hayase received his Ph.D. degree in science from Kyoto University in 2014. After a one-year post-doctoral fellowship, he was an assistant professor at Tohoku University from 2015 to 2019. Since 2019, he has been an Independent Scientist at National Institute for Materials Science. His research interests include fabrication methods for flexible porous materials and their applications.